

AD723434



AD

AMMRC CR 71-4/1

NONDESTRUCTIVE TESTING USING TRW ACOUSTO-OPTICAL IMAGING SYSTEM

January 1971

Robert Aprahamian
Jerold L. Jacoby
Pravin G. Bhuta

Applied Mechanics Laboratory
TRW SYSTEMS GROUP
One Space Park
Redondo Beach, California

SEMI-ANNUAL REPORT - CONTRACT DAAG46-70-C-0103

D D C
REF ID: A65116
MAY 17 1971
D

This document has been approved for public release and sale; its distribution is unlimited.

Prepared for

ARMY MATERIALS AND MECHANICS RESEARCH CENTER
Watertown, Massachusetts 02172

Unclassified

Security Classification

14. KEY WORDS	LINK A		LINK B		LINK C	
	ROLE	WT	ROLE	WT	ROLE	WT
Ultrasonic Frequencies Acoustics Nondestructive Tests Images						

Unclassified

Security Classification

Unclassified

Security Classification

DOCUMENT CONTROL DATA - R & D

(Security classification of title, body of abstract and indexing annotation must be entered when the overall report is classified)

1. ORIGINATING ACTIVITY (Corporate author)

TRW INC.

TRW Systems Group

One Space Park

Redondo Beach, California

2a. REPORT SECURITY CLASSIFICATION

Unclassified

2b. GROUP

NONDESTRUCTIVE TESTING USING TRW ACOUSTO-OPTICAL IMAGING SYSTEM

4. DESCRIPTIVE NOTES (Type of report and inclusive dates)

Semi-Annual Report 30 June 1970 to 30 December 1970

5. AUTHOR(S) (First name, middle initial, last name)

Robert Aprahamian

Jerold L. Jacoby

Pravin G. Bhuta

6. REPORT DATE

January 12, 1971

7a. TOTAL NO. OF PAGES

7b. NO. OF REPS

5

8a. CONTRACT OR GRANT NO.

DAAG46-70-C-0103

8b. ORIGINATOR'S REPORT NUMBER(S)

8c. PROJECT NO.

AMMRC CR 71-4/1

9c. ARPA Order No. 1245

9d. OTHER REPORT NO(S) (Any other numbers that may be assigned this report)

71/4341/9

10. DISTRIBUTION STATEMENT

This document has been approved for public release and sale; its distribution is unlimited.

11. SUPPLEMENTARY NOTES

Sponsored by
Advanced Research Projects Agency

12. SPONSORING MILITARY ACTIVITY

Army Materials and Mechanics Research
Center, Watertown, Massachusetts 02172

13. ABSTRACT

The technique of Acousto-Optical Imaging (AOI) enables one to "see", on a real-time basis, within optically opaque materials and to detect internal or surface flaws and/or other irregularities which might be present. The process uses an ultrasonic beam to probe the object under study. As it interacts with the object, the ultrasonic beam acquires an acoustical "picture" of the object. The acoustic waves then interact with a monochromatic light beam (as from a laser). Optical sidebands are produced by the Bragg diffraction of light. The cumulative result of this process is that these sidebands produce a visual image of the interior of the object. This paper discusses the results of an experimental study to evaluate the applicability of acousto-optical imaging to nondestructive testing. In addition to the determination of the system resolution, the effects of specimen thickness, geometry, composition and surface roughness are under investigation. A new technique which utilizes the sound reflected from the specimen to obtain an acousto-optical image was also developed. Preliminary results utilizing this technique to detect surface flaws on a specimen are encouraging.

DD FORM 1 NOV 65 1473

REPLACES DD FORM 1473, 1 JAN 64, WHICH IS
OBsolete FOR ARMY USE.

Unclassified

Security Classification

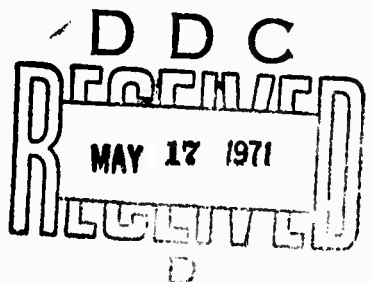
AMMRC CR 71-4/1

NONDESTRUCTIVE TESTING USING TRW ACOUSTO-OPTICAL IMAGING SYSTEM

Robert Aprahamian
Jerold L. Jacoby
Pravin G. Bhuta

Applied Mechanics Laboratory
TRW SYSTEMS GROUP
One Space Park
Redondo Beach, California

Semi-Annual Report - Contract DAAG46-70-C-0103
AMCMS Code 5910.21.66009



This document has been approved for public release and sale; its distribution is unlimited.

Sponsored by
Advanced Research Projects Agency

Prepared for

ARMY MATERIALS AND MECHANICS RESEARCH CENTER
Watertown, Massachusetts 02172

ARMY MATERIALS AND MECHANICS RESEARCH CENTER

NONDESTRUCTIVE TESTING USING
TRW ACOUSTO-OPTICAL IMAGING SYSTEM

ABSTRACT

The technique of Acousto-Optical Imaging (AOI) enables one to "see", on a real-time basis, within optically opaque materials and to detect internal or surface flaws and/or other irregularities which might be present. The process uses an ultrasonic beam to probe the object under study. As it interacts with the object, the ultrasonic beam acquires an acoustical "picture" of the object. The acoustic waves then interact with a monochromatic light beam (as from a laser). Optical sidebands are produced by the Bragg diffraction of light. The cumulative result of this process is that these sidebands produce a visual image of the interior of the object. This paper discusses the results of an experimental study to evaluate the applicability of acousto-optical imaging to nondestructive testing. In addition to the determination of the system resolution, the effects of specimen thickness, geometry, composition and surface roughness are under investigation. A new technique which utilizes the sound reflected from the specimen to obtain an acousto-optical image was also developed. Preliminary results utilizing this technique to detect surface flaws on a specimen are encouraging.

FOREWORD

This report was prepared by the Applied Mechanics Laboratory of TRW Systems Group, Redondo Beach, California under Army Materials and Mechanics Research Center (AMMRC) Contract Number DAAG46-70-C-0103 (ARPA Order Number 1245). Mr. O. R. Gericke served as the technical monitor for AMMRC. Program Manager at TRW Systems was Mr. R. Aprahamian. Technical Support was contributed by Mr. J. L. Jacoby, Dr. P. G. Bhuta and Mr. C. V. Murrow.

CONTENTS

	Page
ABSTRACT	ii
FOREWORD	iii
INTRODUCTION.	1
SYSTEM EVALUATION	2
TEST SPECIMENS.	4
RESOLUTION MEASUREMENTS	5
REFLECTED SOUND IMAGING	16
CONCLUSIONS	22
REFERENCES.	23

INTRODUCTION

The technique of Acousto-Optical Imaging (ACI) enables one to "see", on a real-time basis, within optically opaque materials and to detect internal or surface flaws and/or other irregularities which might be present. The process uses an ultrasonic beam to probe the object under study. As it interacts with the object, the ultrasonic beam acquires an acoustical "picture" of the object. The acoustic waves then interact with a monochromatic light beam (as from a laser). Optical sidebands are produced by the Bragg diffraction of light. The cumulative result of this process is that these sidebands produce a visual image of the interior of the object.

It is the objective of the present study to determine the general applicability of the TRW Acousto-Optical Imaging system to nondestructive testing. This includes experimental study of the capabilities and physical limitations of the Bragg Refraction method which forms the underlying principle of the system. In addition, the ability of the AOI device to image using reflective sound is being investigated. During the first six months of this study, progress has been made in the following areas:

- o System Evaluation

Those factors which influence the performance of the system have been identified. Attempts are being made to vary parameters so as to optimize the system.

- o Test Specimens

Test specimens to measure the system resolution have been fabricated. A new technique for making flawed specimens is under development. This involves casting the "flaw" into a resin material.

- o Resolution Measurements

Images of a series of closely spaced drill holes were photographed. The frequencies were varied from 4 to 40 MHz. The resolution was defined as the ability to distinguish the individual holes. The results are in good agreement with the theoretical predictions for the resolution.

- o Reflective Sound Imaging

Initial tests were begun to obtain an acousto-optical image using the sound reflected from the object. Pulsed light and sound sources were synchronized to "range-gate" the object. In addition, a closed-circuit television system was used to display the images. Images were obtained of a surface flaw on a sample of borsic aluminum.

SYSTEM EVALUATION

The first stage of the program has been used to evaluate the present Acousto-Optical Imaging system.¹ A thorough understanding of the operating characteristics and the relationship between the actual and theoretical performance is prerequisite to further development. It is also necessary to identify those factors which can be used to measure the system performance. Two such parameters are sensitivity and resolution which are a measure of the ability of the system to detect a flaw in a specimen.

Four factors influence the sensitivity of the system: the intensity of the light source (laser), I_o ; the interaction distance between the light and sound, ℓ ; the efficiency of the coupling medium², M_w^* ; and the intensity of the sound in the volume of the light-sound interaction, P_s . These factors are related in the system according to Equation 1:²

$$I = I_o \sin^2 (1.4 \ell \sqrt{M_w P_s}) \quad (1)$$

In order to produce a usable image, a sufficient amount of light must be diffracted into the first sideband. The minimum intensity, I , (Eq. 1) which can be observed visually as a real-time image is³

$$I_{min} = 2.2 \times 10^{-6} \text{ watts/cm}^2$$

The quartz crystals used with this system produce a collimated acoustic wave. The maximum interaction distance, ℓ , is the width of the acoustic column. The efficiency of the coupling medium is given by the figure of merit, M_w . As is seen in Table I, the figure of merit may vary over a large range of values, however, it happens that water is a very good coupling medium. The sound intensity is determined by the output of the sound source (transducer) and the energy loss before the sound reaches the interaction area.

$$*M_w = n^2 p^2 / v \rho$$

n = refractive index of the coupling medium

p = elastooptic coefficient

v = sound velocity

ρ = density

TABLE I²

**Comparison of the Efficiency of the
Coupling Medium for Various Materials**

<u>Material</u>	<u>M_w</u>
Water	1.0
Dense Flint Glass	0.06
Extra-Dense Flint Glass	0.12
Fused Quartz (SiO_2)	0.006
Polystyrene	0.8
KRS-5	1.6
Lithium Niobate (LiNbO_3)	0.012
Lithium Flouride (LiF)	0.001
Rutile (TiO_2)	0.001
Sapphire (Al_2O_3)	0.001

The resolution of an Acousto-Optical Imaging system is ultimately limited by diffraction effects in both the acoustic and optical waves. Factors influencing the resolution include the arrangement of the optical system, the arrangement of the object in the acoustic medium relative to the interaction volume, the size and shape of the interaction volume and the acoustic wavelength.

All of the above factors for determining the sensitivity and resolution of the system can be divided into two groups. The first of these two groups influence the design of the AOI system. When these factors are optimized and built into the system, we expect that they will remain relatively constant. These factors would include the intensity of the light source, the maximum power available to drive the transducer, the coupling medium (water), and the size and shape of the light-sound interaction volume. This last item can be altered by providing the ability to change optical components, however, by proper design this need could be minimized.

The second group of system variables relate not to the construction of the system, but how it is to be used to perform a particular function. For example, the sensitivity is, in part, determined by the sound intensity at the interaction volume. The attenuation of the sound in the water medium is therefore a major factor in determining the sensitivity. (The

characteristic attenuation distance of a 11 Megahertz acoustic wave in water at 20°C is 6 in.)⁴ The sound intensity decreases with the distance

and the square of the frequency ($I = I_0 e^{-\alpha(v^2)x}$). Thus, it would appear that greater sensitivity can be obtained by placing the transducer close to the light-sound interaction volume (if object geometry permits) and by using lower frequency sound. The resolution of an acoustic system is dependent on the acoustic wavelength. The resolution can be increased by using sound having a shorter wavelength, i.e., higher frequency. But this violates our sensitivity condition. Clearly, to optimize the system performance, a tradeoff between these two requirements must occur. This can be accomplished by taking into account the attenuation for a particular situation and the resolution required.

TEST SPECIMENS

In order to properly evaluate the capabilities and limitations of an imaging system, it is necessary to have a set of standards such that the data can be expressed in quantitative form. Tests using naturally occurring flaws in materials are valid only to the extent that the character of the flaw can be verified by alternate methods. This approach, however, is subject to the limitations of the other systems. In some cases, it may be difficult to find flawed specimens exhibiting the desired characteristics. A more positive approach to this problem is to fabricate control specimens which have the desired specifications.

Two specimens were designed for use in determining the resolution of the AOI system. The specimens are flat aluminum plates (0.125" thick) with a series of holes drilled into them from one side, Figure 1. The hole diameters are 0.110", 0.055", 0.028" and 0.0135". One specimen has one hole of each size while the other has four holes of each size. The separation between these holes is equal to the hole diameter. Tolerances on these specimens were held to $\pm 0.001"$.

Machining artificial flaws and defects, such as the drilled holes in Figure 1, is a very precise technique. However, certain size and geometrical limitations are encountered. Future tasks of this study require that very small defects be used to determine the minimum flaw size which can be detected. It is also desired to investigate the three-dimensional character of flaws. A new technique for fabricating test specimens containing precisely known flaws is being investigated. Lengths of thin wire and small three-dimensional objects will be cast into resin blocks. Tests are presently being made to find a resin, or similar material, which is sufficiently transparent to high frequency ultrasound. The objects cast into the resin will scatter sound in the same way as a flaw. This technique will allow the "flaws" to be precisely measured before the casting is made. In addition, many of these materials

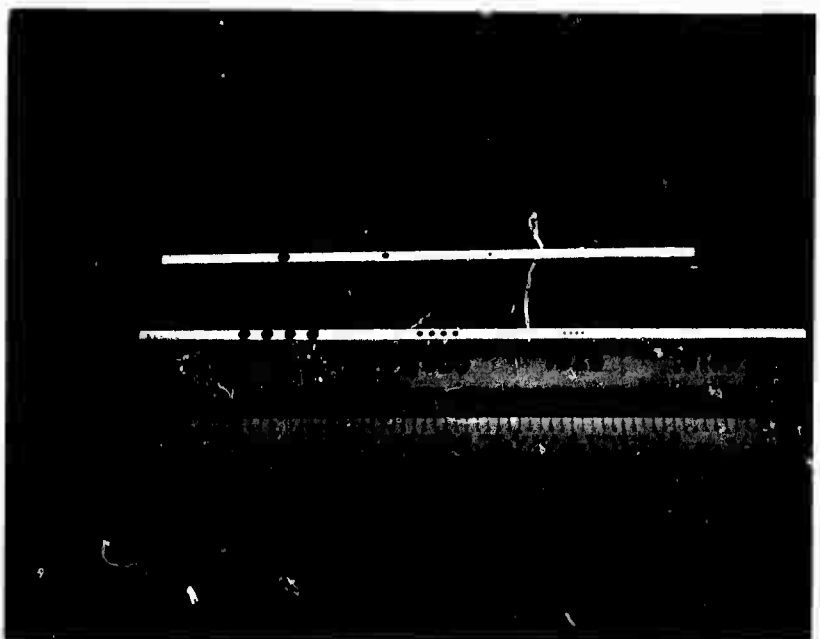


Figure 1: Calibrated Test Specimens. Hole diameters (in inches) are indicated below each set of holes.

are optically transparent. This would allow the "flaw" to be examined and measured after it is cast.

RESOLUTION MEASUREMENTS

The actual evaluation and reporting of the resolution creates somewhat of a problem. For real-time measurement, the operator must make a subjective evaluation of the image. Resolving a clear well-focused image of a flaw is more difficult than simply detecting its existence. For the purpose of this study, we have arbitrarily defined the resolution as being the smallest set of drill holes in our calibration specimens, where the images of the individual holes remain distinguishable. This specimen, shown in Figure 1, consists of four sets of four holes. The spacing between the holes in each set is equal to the hole diameter.

While the outstanding feature of the AOI system is that it produces real-time images, it is also necessary that a good photographic record be obtained. This is the only way in which test results can be reported and compared. Difficulties in photographing images are often encountered when laser light is used (as in holography). This is a consequence of the granular nature of laser light. It is often found that a good, real-time image will not produce a good photograph. In other cases, the photograph is better. A variety of different photographic techniques have been applied to the recording of AOI images. These have included a number of different optical arrangements, cameras, films and development processes. One of the more successful techniques and by far the easiest and fastest involves the use of Polaroid film. The screen which is normally used to display the real image is replaced by the film packet. The packet is opened in the darkened room and the laser shuttered to provide the proper exposure. The film is exposed directly by the AOI image. No "camera" or other focusing optics are needed. The images presented in this section were recorded by this method on Polaroid Type 52 and Type 55 P/N films (type 55 P/N provides both a positive print and a negative).

Two x-cut quartz transducers, measuring about 1-1/4" square, were used for these tests. Their fundamental frequencies were 4 MHz and 8 MHz. These transducers can be operated at their fundamental frequencies and at their odd harmonics. Thus, the 4 MHz transducer was used at 4, 12, 20 and 28 MHz and the 8 MHz transducer was used at 8, 24 and 40 MHz. Images of the four sets of holes at each of these frequencies were obtained and are presented in Figures 2 through 5. Each figure shows a different set of holes imaged at the available frequencies. (Note that the smallest holes, Figure 5, could not be resolved at the lower frequencies and so these pictures were omitted.)

The ability to resolve the images is limited by two effects, (i) the resolution of the light-sound interaction and (ii) the diffraction of the sound due to the small drilled holes in the specimen. From Reference 5, the theoretical resolution limit, d , for the light-sound interaction is given by

$$d = (2n/\pi\phi)\lambda \quad (2)$$

n = index of refraction of water

ϕ = light cone divergence angle
(.093 radians for our tests)

λ = acoustic wavelength in water

In this equation, d is defined as the minimum resolvable linear ultrasonic dimension in the plane orthogonal to the line axis of the light beam,

4 MHz crystal transducer

a. 4 MHz



c. 12 MHz



d. 20 MHz



f. 28 MHz

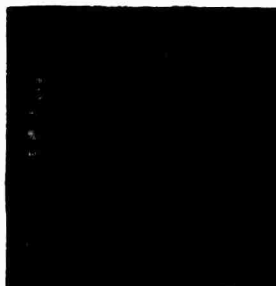


8 MHz crystal transducer

b. 8 MHz



e. 24 MHz



g. 40 MHz



Figure 2. Acousto-Optical Images at Various Frequencies
of Four 0.110" Diameter Holes

4 MHz crystal transducer

a. 4 MHz



c. 12 MHz



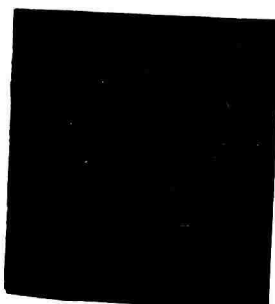
d. 20 MHz



f. 28 MHz

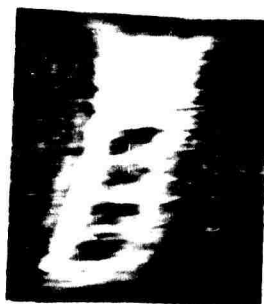


g. 40 MHz



8 MHz crystal transducer

b. 8 MHz



e. 24 MHz



Figure 3. Acousto-Optical Images at Various Frequencies
of Four 0.055" Diameter Holes

4 MHz crystal transducer

a. 4 MHz



c. 12 MHz



d. 20 MHz



f. 28 MHz



8 MHz crystal transducer

b. 8 MHz



e. 24 MHz



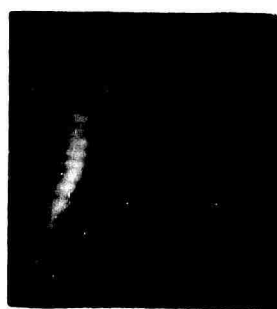
g. 40 MHz



Figure 4. Acousto-Optical Images at Various Frequencies of Four 0.028" Diameter Holes

4 MHz crystal transducer

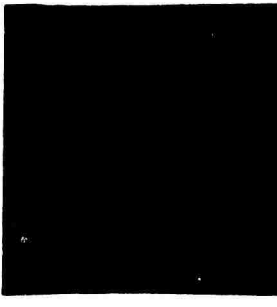
a. 12 MHz



b. 20 MHz



d. 28 MHz



8 MHz crystal transducer

c. 24 MHz



e. 40 MHz

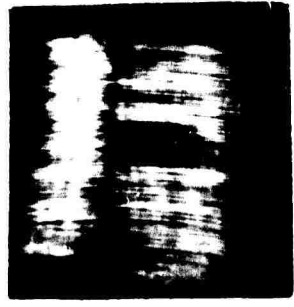


Figure 5. Acousto-Optical Images at Various Frequencies
of Four 0.0135" Diameter Holes

(i.e., d is the theoretical resolution along the vertical axis of the images in Figures 2-5.) Recalling that we have equated the ability to resolve an image with the ability to distinguish the individual drill holes, Equation 2 can be evaluated with the aid of Figures 2-5. For example, for a frequency of 4 MHz, the theoretical resolution limit, d , is 0.1310". The largest hole diameters are 0.110". As this is smaller than d , one would not expect to be able to resolve a clear image of any of the holes at this frequency. This lack of resolution is evident in the Figures. At 12 MHz, the theoretical resolution is 0.0437". As expected, the 0.110" diameter holes are clearly resolved. The images of the 0.055" and the 0.028" diameter holes show diffraction effects. It is difficult to distinguish the hole boundaries and it appears that five or more holes are present. (This is discussed in greater detail below.) The 0.0135" diameter holes are not resolved at this frequency.

The resolution limit, d , (from Equation 2) is plotted vs. acoustic frequency in Figure 6. The resolution of the images in Figures 2 through 5 were rated by several individuals within the laboratory. The position where each image falls on the graph in Figure 6 has been noted by its rating: (G = Good; F = Fair, P = Poor). Equation 2 predicts that we will be able to resolve the drill holes in those images which fall above the line in Figure 6. For the images below the line, it is expected that the drill holes would be indistinguishable. It can be seen from Figures 2-5 that our results are in general agreement with these predictions.

In several of the images, in particular, those which fall near the line in Figure 6, it is difficult to determine the boundaries of the holes. In some of the pictures, it appears that more than four holes are present. These effects are due to the diffraction of the sound in the specimen. Diffraction effects are not important as long as $\lambda_s/a \ll 1$ (where λ_s is the acoustic wavelength in the specimen and a is the hole diameter). For these experiments, λ_s is on the same order as a and thus the diffraction of sound by the drilled holes is a significant factor in the resolution of the system.

To determine the effects of acoustic scattering, we will compare the size of one set of holes as determined from the acousto-optical image with the actual specimen. For this purpose, we choose to consider the 0.055" diameter holes imaged with 24 MHz sound, as shown in Figure 3e. To arrive at the size of the holes from the acousto-optical image, one must consider the magnification inherent in the acousto-optical imaging process. The magnification factor is obtained by measuring the distance between the center lines of the two outer holes and comparing it with the actual distance between the holes as measured from the specimen, see Figure 7. The magnification factor is given by the ratio of the image size to the actual specimen size and is found to be

$$M = \frac{\text{Image Size}}{\text{Specimen Size}} = \frac{0.53 \pm 0.02"}{0.330" \pm 0.001"} = 1.6 \pm 0.1$$

G = Good
F = Fair
P = Poor

$$d = \frac{2\pi}{\pi\phi} \lambda = \frac{2\pi v}{\pi\phi v}$$

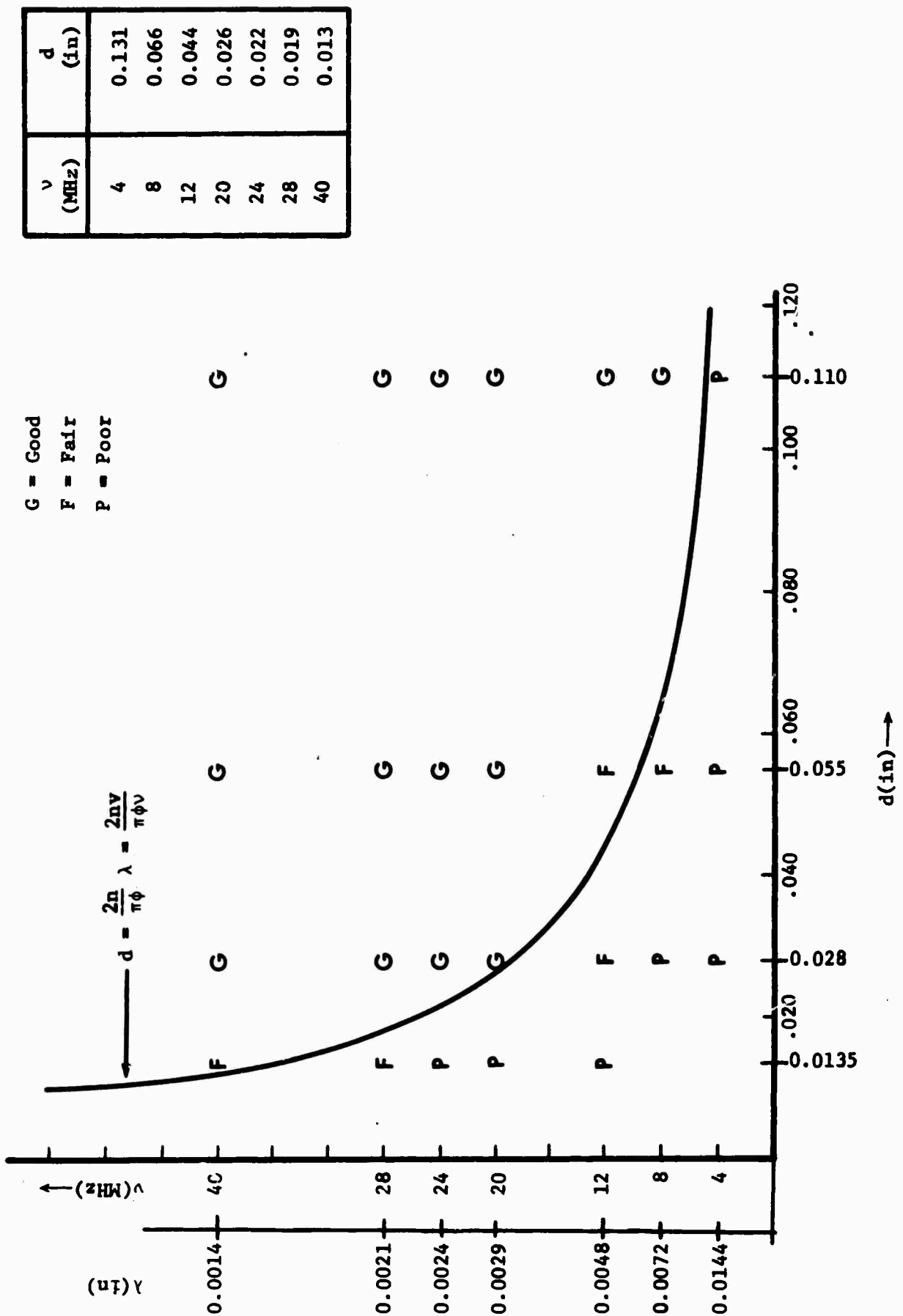
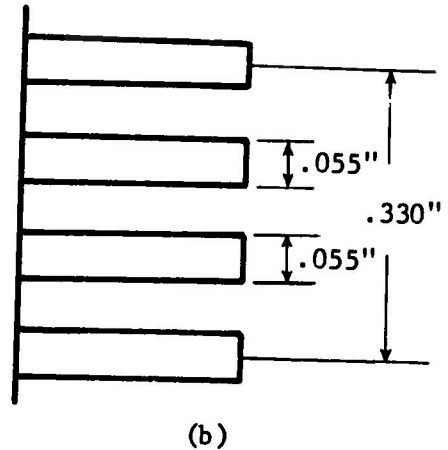


Figure 6: Resolution limit, d, vs. acoustic frequency, v. The letters indicate the appropriate positions of the images in Figures 2-5 and signify the quality of each image



(a)



(b)

Figure 7: Comparison of AOI image with actual specimen dimension for .055" diameter holes imaged at 24 MHz

(a) Acousto-optical Image

(b) Schematic of actual specimen

The error band, $\pm 0.02"$, assigned to the acousto-optical image measurement is obtained from the optical resolution limit, d , discussed previously (Equation 2). The tolerance $\pm .001"$ is the tolerance held by the machinist in fabricating the specimen. Having this magnification factor, the hole diameter measured from Figure 7a can be determined to be

$$\text{AOI hole size} = \frac{0.11" \pm 0.02"}{1.6 \pm 0.1} = .069" \pm .017"$$

where again the error band ± 0.02 is attributed to the optical resolution limit given by Equation 2. The actual size of the hole falls within the range of this figure.

To determine the magnitude of the diffraction effects, we will next consider the case of Fresnel diffraction of plane acoustic waves by a single narrow opaque strip of infinite length as depicted in Figure 8. It can be shown (Ref. 6) that the intensity distribution describing this situation is given by

$$I(x_0) = \frac{1}{4} \left[1 + \left[C(\xi_1) - C(\xi_2) \right]^2 + \left[S(\xi_1) - S(\xi_2) \right]^2 + 2 \left[C(\xi_1) - C(\xi_2) \right] \right] \quad (3)$$

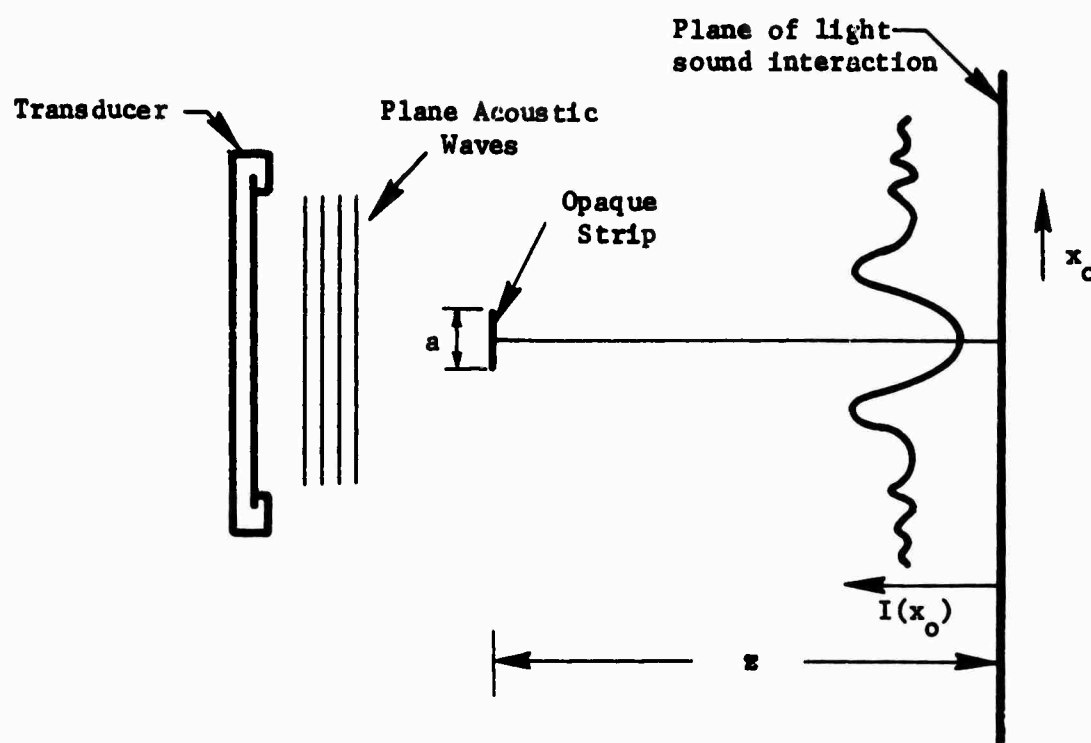


Figure 8: Schematic representation of plane sound waves being diffracted by an infinitely long (out of page) opaque strip of width a . A typical intensity function is shown plotted opposite the strip.

where $C(\xi)$ and $S(\xi)$ denote the Fresnel Integrals defined by

$$C(\xi) = \int_0^\xi \cos \frac{\pi t^2}{2} dt \quad (4)$$

$$S(\xi) = \int_0^\xi \sin \frac{\pi t^2}{2} dt$$

and

$$\xi_1 = -\sqrt{\frac{2}{z\lambda_s}} \left(\frac{a}{2} + x_0 \right)$$

$$\xi_2 = \sqrt{\frac{2}{z\lambda_s}} \left(\frac{a}{2} - x_0 \right)$$

The intensity distribution, $I(x_0)$, given by Equation 3 was solved numerically by a computer for our experimental configuration, viz

$$\lambda_s = 0.007"$$

$$a = 0.055"$$

$$z = 1.0"$$

$I(x_0)$, as plotted by the computer, is shown in Figure 9. The range of x_0 on this plot is $x_0 = \pm 0.250"$. The width of the central minimum measured between points B on the diagram is $0.096" \pm .005"$. This is larger than the measured width of the hole image ($0.069" \pm .017"$). It is expected that this discrepancy is due to the use of single opaque strip model rather than a four opaque strip model which would more accurately describe the actual specimen. During the next reporting period, this model will be run on the computer.

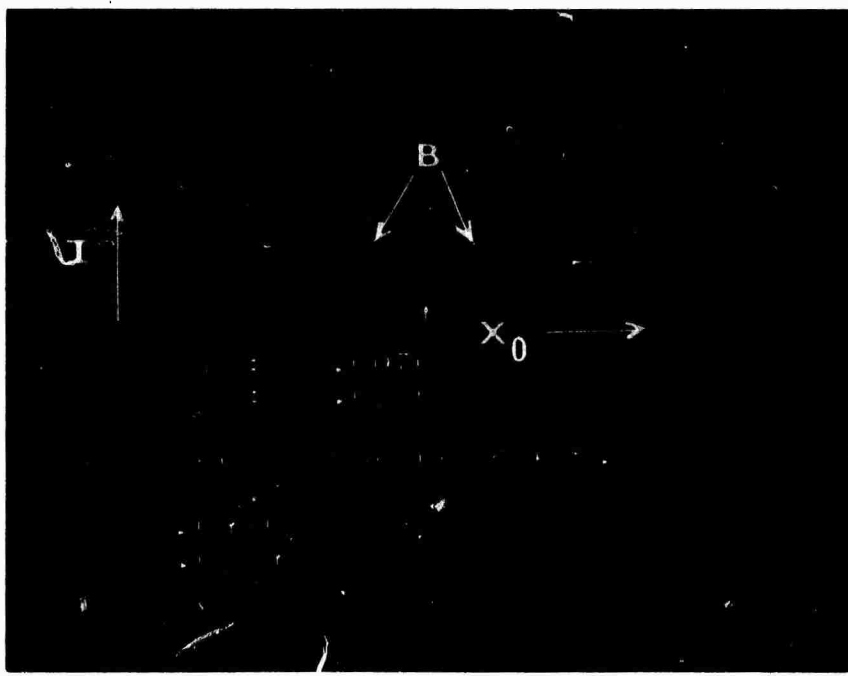


Figure 9: Computer generated intensity distribution for the diffraction of 24 MHz plane acoustic waves by an opaque strip of width 0.055". The range of x_0 is $\pm 0.250"$. The acoustic wavelength in the specimen is $0.007"$. The width of the central minimum measured between points B is $0.096" \pm .005"$. The width of the central minimum at one-half of this intensity is $0.076" \pm .005"$.

In summary, the following measurements were made of the .055" diameter hole imaged at 24 MHz

<u>Method of Measurement</u>	<u>Measured Hole Diameter</u>
Actual Specimen Size	0.055" \pm .001"
Measurement from AOI Image	0.069" \pm .017"
Calculation of Single Opaque Strip Diffraction Pattern	0.096 \pm .005"

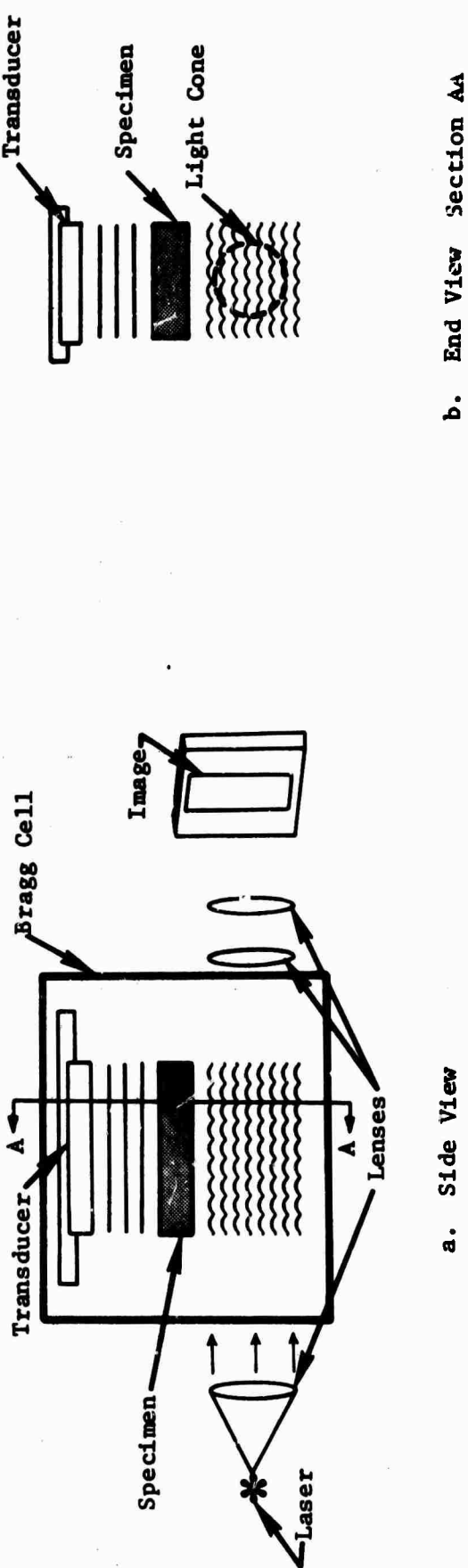
REFLECTED SOUND IMAGING

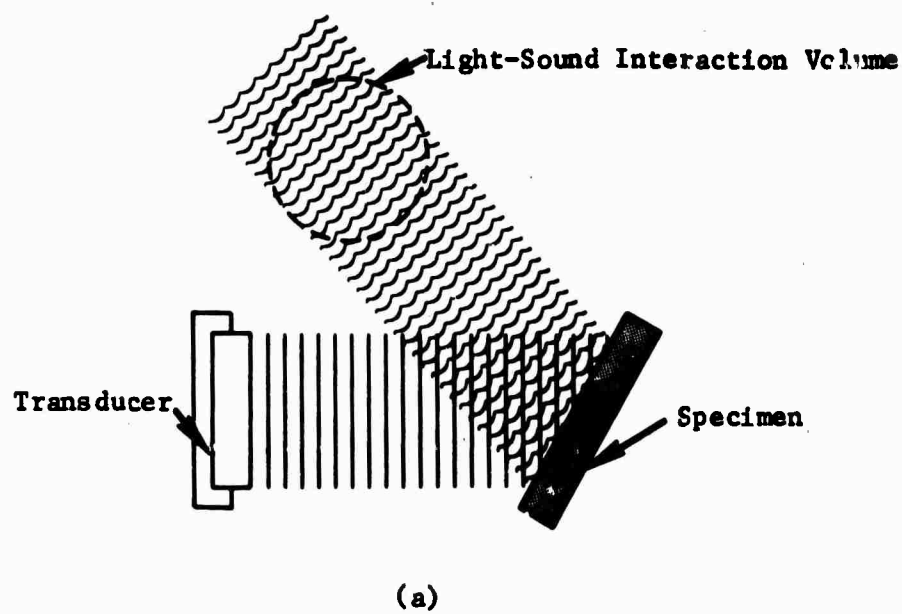
Previous work with the acousto-optical imaging (AOI) system used transmitted sound waves to probe the material being inspected, i.e., the acoustic waves were passed through the specimen. In this configuration, illustrated in Figure 10, the crystal transducer (used to generate the acoustic energy) is placed on one side of the specimen and emits a plane acoustic wave which interacts with the specimen. That part of the wave which is transmitted through the specimen is distorted so that it carries with it an acoustic image of the interior of the specimen. Light is then Bragg diffracted from the acoustic wave. A real-time image of the interior of the specimen is thus projected onto a viewing screen.

In many cases, access to both sides of a specimen is not possible and therefore the ability to inspect parts from one side is desirable. This can be done by placing the transducer and the light-sound interaction volume on the same side of the specimen and using the sound which is reflected from the specimen to form an image. Experiments were performed in an effort to demonstrate this technique. Initially, the feasibility of using reflected sound to detect surface cracks was investigated. In conjunction with the use of reflected sound, two other new techniques were employed. They were the use of pulsed light and sound sources and the use of a closed-circuit television system to intensify and enlarge the image.

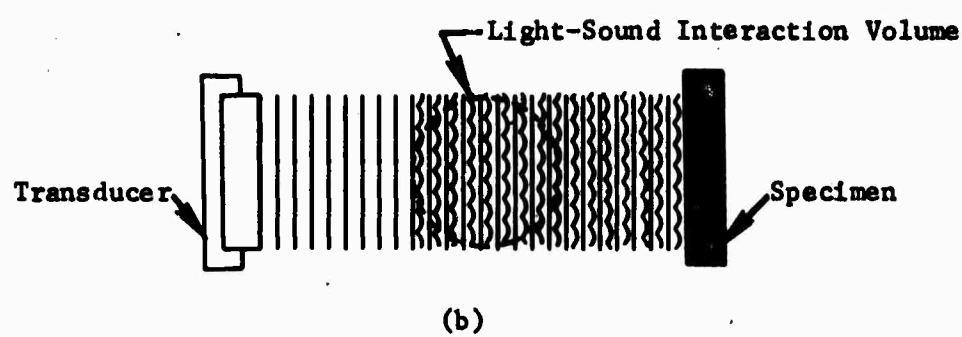
A continuous wave (cw) sound source can be used for reflected sound imaging if the proper experimental geometry is employed. An example of a possible experimental arrangement is shown in Figure 11a. For these tests, however, a preferred arrangement is with the sound wave incident normally with the specimen. The experimental arrangement used is very simple, however, the sound must travel twice through the light-sound interaction volume. (See Figure 11b.) This arrangement produces two images if continuous light and sound sources are used. As the sound travels from the transducer to the specimen, through the interaction volume, an image of the transducer is formed. In the second step, the

Figure 10: Experimental configuration for acousto-optical imaging where sound is transmitted through the specimen





(a)



(b)

Figure 11: Two possible experimental configurations
for reflective sound imaging

reflected sound travels again through the interaction volume producing a second image. This problem can be overcome by turning off the light during step 1 and turning off the sound source during step 2, i.e., using properly phased pulsed light and sound sources. A pulsed oscillator was used to provide sound pulses of 25 μ sec duration at a rate of 60 pps. The laser was a TRW Instruments pulsed argon laser (5145 \AA and 4880 \AA) producing pulses of 40 μ sec duration at a rate of 60 pps. While the duty cycle is very low for this mode of operation, the higher peak powers obtained from both the light and sound sources combine to produce an average image intensity only slightly less than in the cw mode when a 15 mw laser is used. Pulsing the sound source also prevents the occurrence of standing waves in the tank.

It was necessary to initiate the light pulse after the sound so that both the light and sound would arrive at the interaction volume simultaneously. The oscillator provided a delayed trigger signal which was used to trigger the laser. This delay is continuously variable from 2 μ sec to 2 msec. Referring to Figure 12, a delay of $t = A/v$, where v represents the velocity of sound, would allow the sound coming directly from the

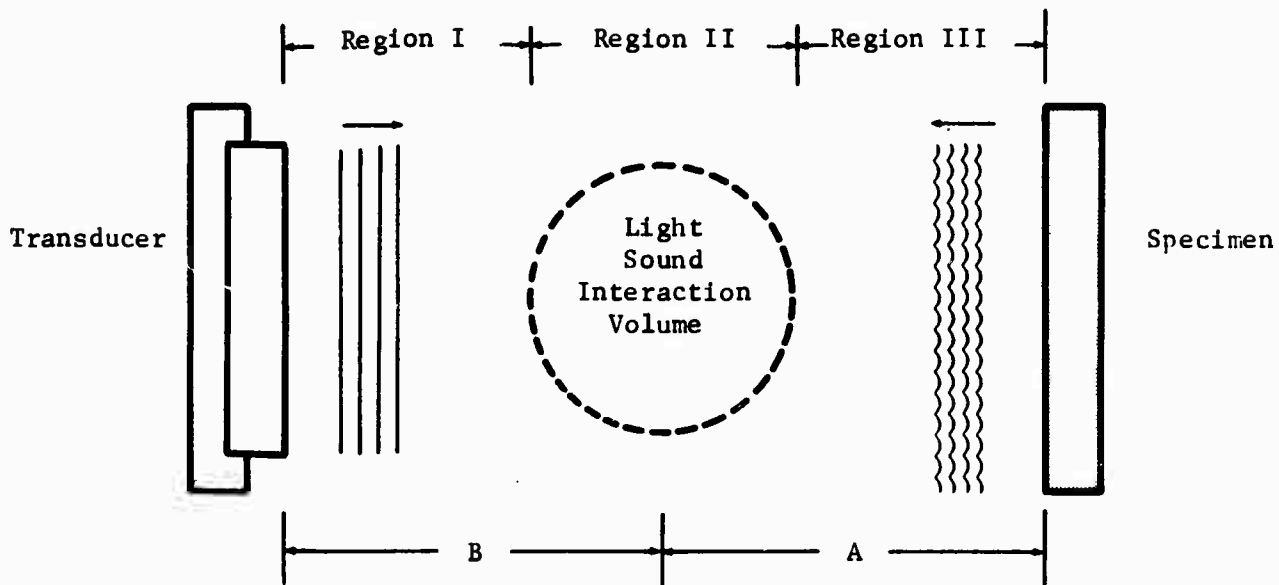


Figure 12: Experimental configuration for reflective sound imaging using pulsed light and sound sources.

transducer to be imaged. At this setting, a specimen situated in region I could be inspected by the transmission method. By adjusting the laser delay to $t = (A + 2B)/v$, an image would be formed by the sound being reflected from a specimen in region III. (The delay due to the speed of light is negligible.)

The first tests with this system were made using the transmission mode of operation so that the image quality could be compared with that obtained using continuous wave light and sound sources. It was found that a double, or "ghost" image was obtained because of the two principal wavelengths of light present. The problem could be eliminated by filtering out all but the 5145A component of the light. While the proper filter was not available in the laboratory, a filter was obtained which provided a usable image. The pulsed images appeared to have better contrast ratios than those obtained with the cw mode. This is possibly due to the higher sound intensities which created a more efficient diffraction pattern. This also aided in imaging thicker materials in which the sound is attenuated. The only disadvantage encountered was the low overall intensity of the image. This problem was overcome by the use of a closed circuit television system. The real acousto-optical image was projected directly onto the face of the vidicon tube of a television camera. The image was then viewed on a 21" diagonal television monitor. This not only produced a brighter image but the larger size enabled greater detail to be seen. Figure 13 shows the experimental setup with the closed circuit television system.

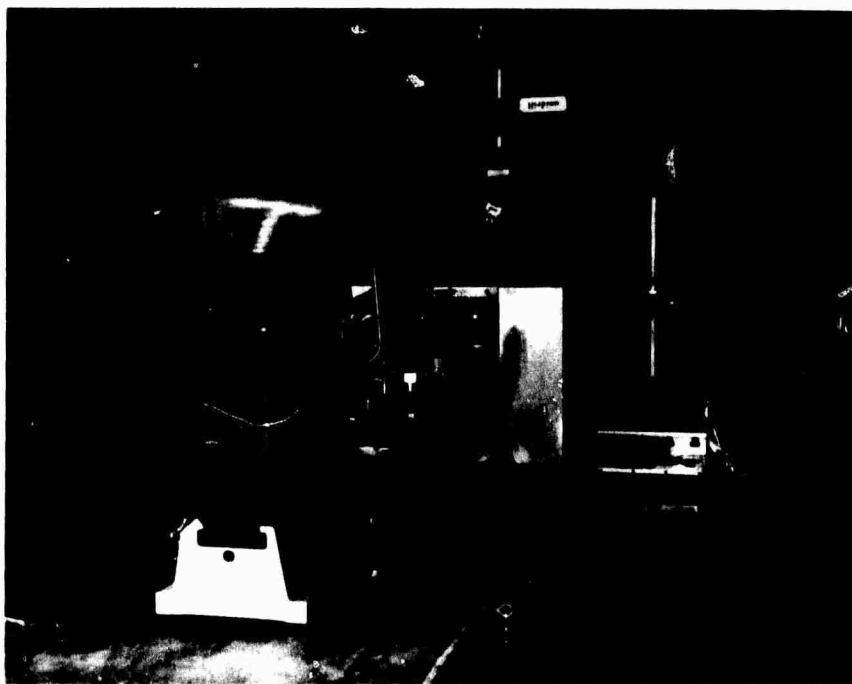
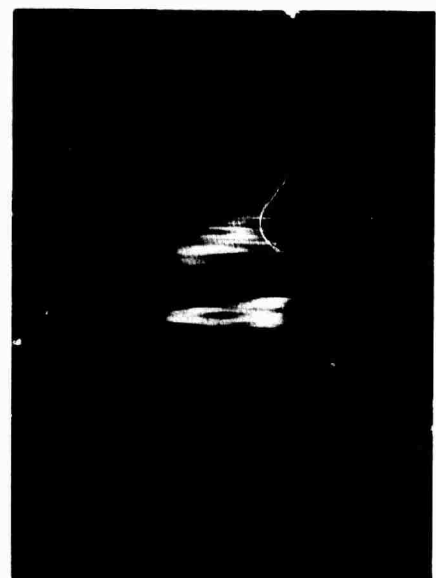


Figure 13: Experimental setup showing closed circuit television system

A specimen of borsic aluminum containing a surface flaw was positioned opposite the transducer (Region III in Figure 12). By careful orientation of the specimen, it was possible to reflect the sound off its front surface and obtain an image of the transducer. As the flawed area was moved into the acoustic wave, a corresponding gap in the transducer image moved through the field of view. The images derived from the acoustic wave which was reflected from the flawed and nonflawed portions of the specimen are shown in Figure 14. These are pictures of the television monitor which was displaying the images. A photograph of the flawed specimen is shown in Figure 15.



(a) Unflawed specimen section



(b) Reflected image showing flaw

Figure 14: Reflected sound images of specimen of borsic aluminum containing surface flaw



Figure 15: Flawed section of borsic aluminum specimen

Further tests will investigate the applicability of these techniques to the imaging of internal flaws in the specimen. It is necessary to eliminate the acoustic wave which is reflected from the front surface of the specimen from that which carries the signal from inside the specimen. This requires that the acoustic pulse length ($\Delta L = v\Delta t$) be smaller than twice the flaw depth. Much shorter acoustic and light pulse durations are required than used for the tests discussed above. To meet these requirements, TRW is presently constructing a new pulsed xenon laser using company capital funds. This laser will provide pulse durations as short as one microsecond. The peak power will be about 100 watts with a nominal repetition rate of 100 pps. The pulsed oscillator already has the capability of short pulse durations. It is expected that the new laser will be operational within the next two months. It is also worthwhile to note that proper timing and phasing of the light and sound waves will allow for the use of range gating techniques to determine the depth of the flaw in the specimen.

CONCLUSIONS

Test specimens were fabricated for measuring the resolution of the acousto-optical imaging system. These consisted of sets of four closely

spaced holes of varying diameters. The resolution was defined as the ability to distinguish the individual holes. These holes were imaged using acoustic frequencies ranging from 4 to 40 MHz. The ability to resolve the holes agreed well with the theoretical predictions. As expected, the resolution is proportional to the acoustic frequency. Equation 2 also predicts that the resolution is proportional to the cone convergence angle (i.e., that a larger angle will lower the minimum resolvable distance). Different cone angles will be tried during the next phase of this study.

A system was designed to investigate the use of reflective sound for acousto-optical imaging. Pulsed light and sound sources were used in synchronization so that the object could be "range-gated." Images were obtained in both the transmission and reflection mode by adjusting the relative phasing of the light and sound sources. The image intensities were low due to the low duty cycle of the pulsing. This was overcome by the use of a closed-circuit television system to both amplify and enlarge the visual image. Images of a surface flaw on a specimen of borsic aluminum were obtained with the reflection technique. The applicability of these methods to the imaging of internal flaws will be the subject of further tests. A pulsed xenon laser to be used for this study is currently being fabricated using TRW capital funds.

Further efforts will include an investigation of the effects of specimen geometry and surface roughness on the quality of the acousto-optical image. It will be determined whether the three-dimensional character of the flaw can be determined. Finally, an analysis will be performed to design an acoustic microscope based upon the acousto-optical imaging technique.

REFERENCES

1. R. Aprahamian and P. G. Bhuta, "NDT by Acousto-Optical Imaging," to be published in Material Evaluation, May, 1971.
2. R. Adler, "Interaction Between Light and Sound," IEEE Spectrum, pp. 42-54, May 1967.
3. S. H. Bartley, "The Psychophysiology of Vision," pp 945-948, Handbook of Experimental Psychology, edited by S. S. Stevens, John Wiley & Sons, Inc., New York, 1951.
4. N. E. Dorsey, Properties of Ordinary Water-Substance, Reinhold Pub., 1940, pg 197.
5. C. S. Tsai and H. V. Hance, "Experimental Investigation of the Resolution Capability of Microwave Ultrasonic-Beam Visualization Techniques Using Bragg Diffraction of a Laser Beam," J. Acoust. Soc. Amer. 48, 1110-1118 (1970).
6. J. W. Goodman, Introduction to Fourier Optics, McGraw-Hill, San Francisco, 1968, pp. 70-72.